Recent Developments in Perturbative QCD

Lance J. Dixon

Stanford Linear Accelerator Center, Stanford University, Stanford, CA 94309, USA

Abstract. I review recent progress in perturbative QCD on two fronts: extending next-to-next-to-leading order QCD corrections to a broader range of collider processes, and applying twistor-space methods (and related spinoffs) to computations of multi-parton scattering amplitudes.

Keywords: Perturbative QCD calculations
PACS: 12.38.Bx

A method is more important than a discovery,
since the right method will lead to new and even more important discoveries.
– L. D. Landau

INTRODUCTION

Asymptotic freedom [1], for which Gross, Politzer and Wilczek received the 2004 Nobel Prize in Physics, provides the conceptual framework for applying perturbative QCD to short-distance-dominated problems in hadronic physics, such as the deep-inelastic (DIS) scattering process, the focus of this series of workshops. Supplemented with the notion of factorization [2], and the experimental determination of parton distributions, perturbative QCD has become the basis for all quantitative theoretical predictions for large-transverse momentum processes in hadron-hadron and ep collisions, as well as jet production in e^+e^- annihilation.

One might have thought that by now, with the aid of computers, perturbative QCD should have been "reduced to quadratures", that is, to a simple exercise in tabulating and numerically evaluating Feynman diagrams. Yet it is often the case that the experimental precision exceeds the theoretical uncertainties, due to unknown higher-order terms in the perturbation series. Here I will cover two topics in computational perturbative QCD, for which there has been a great deal of progress, although much still remains to be done.

The first topic concerns next-to-next-to-leading order (NNLO) corrections to collider processes, also the subject of another talk at this workshop [3]. NNLO computations have been available for a limited number of collider observables for many years, but only now are the prospects becoming good for extending them to a broader range of important precision processes at hadron colliders.

The second topic is a rapidly developing one, in which insights gleaned from the topological string in twistor space proposed by Witten [4], and further developments, promise to provide efficient means for computing tree-level and one-loop QCD amplitudes with a large number of external partons, as well as vector and Higgs bosons. These amplitudes are needed for next-to-leading order corrections to a variety of processes.

PROGRESS AT NNLO

For most observables, the QCD perturbation series is a slowly converging one. (Technically it is an asymptotic series, but rarely are there enough terms available in the series for the distinction to matter quantitatively.) Typical next-to-leading order (NLO) corrections for collider processes range from 20% to 100%. Clearly any kind of precision measurement, say at the few percent level, will require the NNLO terms in the series as well. Examples where this precision is desirable include the determination of

- α_s via jet production and event shapes in e^+e^- annihilation (as well as in ep collisions)
- parton distributions via DIS, Drell-Yan production, and high-p_T jet production at hadron colliders
- electroweak parameters, such as M_W, via W and Z production at hadron colliders
- the "partonic luminosity" at the LHC [5]
- Higgs couplings.

The progress of NNLO computations for collider processes can be charted in terms of the number of physical scales present in the parton-level cross sections. The more scales, the more difficult the computation, but the more flexible the applications. In perturbative QCD with massless quarks, all relevant scales are associated with the external kinematics. (The dependence of the partonic cross sections on the renormalization and factorization scales can be determined with relatively little effort, so it can be neglected in this counting.) Also, dimensional analysis can be used to remove an overall dimensionful scale from the problem, leaving just the number of dimensionless ratios.

No-scale problems

For example, in the total cross section for e^+e^- annihilation into hadrons, or equivalently the ratio $R_{e^+e^-}(s) = \sigma(e^+e^- \to \text{hadrons})/\sigma(e^+e^- \to \mu^+\mu^-)$, the only physical scale is s, the square of the center-of-mass energy. This scale can be removed trivially, so $R_{e^+e^-}(s)$ is really a no-scale problem, from the computational point of view. That is, each term in the perturbative series for $R_{e^+e^-}$ is (for fixed renormalization scale μ) a pure number. Related to the lack of other scales in the problem is the totally inclusive nature of the observable; that is, it sums over all hadronic final states with no constraints. This sum can be performed using unitarity, or the optical theorem, as illustrated in fig. 1, transforming the problem into the computation of the imaginary part of the virtual photon propagator, or two-point function.

No-scale processes were the first to be computed at NNLO in perturbative QCD, in the early 1990s. Besides $R_{e^+e^-}$ and the closely related problem of the semi-hadronic width of the τ lepton, $\Gamma(\tau \to \nu_\tau + \text{hadrons})$ [6], various DIS sum rules were also evaluated at this order: the Bjorken sum rule for neutrino scattering, $\int_0^1 dx\,[F_1^{\bar{\nu}p}(x,Q^2) - F_1^{\nu p}(x,Q^2)]$ [7], the Bjorken sum rule for polarized electroproduction, and the Gross-Llewellyn Smith sum rule for neutrino scattering [8]. The integrals over x not only remove dependence

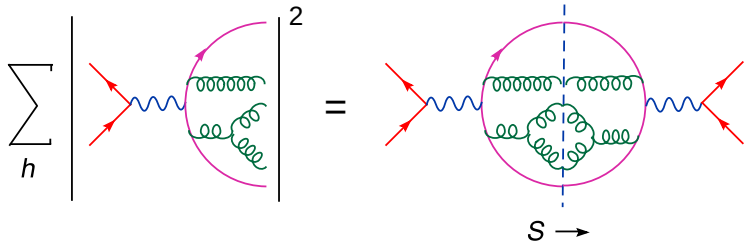

FIGURE 1. Unitarity relates the $e^+e^- \to$ hadrons total cross section to propagator-type loop integrals.

of the observables on parton distribution functions, but they reduce the computation to a no-scale, propagator-type problem very similar to $R_{e^+e^-}$.

The technology underlying all these computations was integration by parts (IBP) [9]. Total derivatives of multi-loop integrals in $D = 4 - 2\varepsilon$ space-time dimensions (*i.e.*, using dimensional regularization), such as

$$\begin{aligned} 0 &= \int d^D p d^D q \ldots \frac{\partial}{\partial q^\mu} \frac{k^\mu}{p^2 q^2 (p+q)^2 \ldots} \\ &= \int d^D p d^D q \ldots \left[- \frac{2k\cdot q}{p^2 [q^2]^2 (p+q)^2 \ldots} - \frac{2k\cdot (p+q)}{p^2 q^2 [(p+q)^2]^2 \ldots} \right], \end{aligned} \tag{1}$$

where p and q are loop momenta, and k is an external momenta, can be re-expressed as linear equations relating loop integrals with propagators raised to different powers. The absorptive parts of four-loop propagators can be related to three-loop propagators via the R^* operation [10]. For the three-loop propagator problem, a recursive solution to the system of linear IBP equations, in terms of a small set of irreducible, "master" integrals, was implemented in the program `MINCER` [11], making possible the previously-mentioned NNLO results.

The pure numbers encountered at NNLO in no-scale problems have a very simple analytic structure. The only algebraic quantities appearing, besides rational numbers, are the Riemann zeta values, $\zeta(n)$, for $n \leq 5$. The results from the early 1990s stood as the computational state-of-the-art for many years. (Very recently, a method for handling the four-loop propagators with all possible topologies has proven successful [12], suggesting that the N^{3}LO results for $R_{e^+e^-}$ may be available before long.) They have led to $\alpha_s(Q^2)$ determinations with the smallest theoretical uncertainty — if Q^2 can be made large enough experimentally, for example, at the Z^0 pole. However, the experimental precision is highly stressed by the leading "1" in $R_{e^+e^-} \propto 1 + \alpha_s/\pi + \cdots$: A 3% measurement of $\alpha_s(M_Z) \approx 0.120$ requires a parts per mil measurement at the Z pole of $\Gamma(Z \to \text{hadrons})/\Gamma(Z \to \mu^+\mu^-)$ [13]. Observables beginning at order α_s, *e.g.*, e^+e^- event-shape variables, are less demanding in this way, motivating their NNLO computation, which is a multi-scale problem, only now approaching completion.

One-scale problems

Also around 1990, the first NNLO computation of a one-scale collider process was carried out, the total cross section for inclusive production in hadronic collisions of a lepton pair via the Drell-Yan process, *i.e.* via a vector boson $V = \gamma^*$, W or Z [14]. At the parton level, the process $pp \to V + X$, where V has mass M_V, introduces the single dimensionless ratio $z \equiv M_V^2/\hat{s}$, where $\hat{s}$ is the squared partonic center-of-mass energy. Whereas the NLO correction to the total cross section was sizable, at NNLO, for W or Z production at the Tevatron or LHC, the perturbative series nicely stabilized.

The NNLO Drell-Yan result was followed quickly by the Wilson coefficient functions $C_i(z)$ for DIS structure functions [15] — except for the longitudinal structure function F_L, which begins at one order higher in α_s, and whose computation was just completed this spring [16].

In the past few years, the NNLO corrections to two additional one-scale collider processes were attacked. First, the total cross section for inclusive production of a Higgs boson in hadronic collisions, $pp \to H + X$ was computed in the large m_t approximation. In this limit, Higgs production is kinematically very similar to the Drell-Yan process, because V and H are both massive color-singlet particles, and no other mass scales remain in the problem — other than the overall Higgs coupling strength, dictated by the operator $C(m_t)H\mathrm{tr}(G_{\mu\nu}G^{\mu\nu})$. Indeed the first Higgs computation, via a high-order expansion in $1-z$ (where now $z = M_H^2/\hat{s}$) [17] was also applied to the Drell-Yan case, revealing a numerically small correction to the original results.

A second Higgs production computation [18] exploited unitarity to express the partonic Higgs cross section as a forward scattering process, as shown in fig. 2. In this case, the state that scatters forward is not a single massive virtual photon, but a pair of massless initial partons. Also, not every cut is considered, but only those that cut through the Higgs particle (or vector boson V). The advantage of this approach is that the large number of phase-space integrals that have to be performed (only one example of which is shown on the left-hand side of fig. 2) can be traded for multi-loop integrals, to which the IBP method can be applied in an automated fashion [19], in order to reduce the integrals to a manageable set of master integrals. In contrast to the no-scale examples, now all the master integrals depend on z. They also depend on the dimensional regularization parameter ε, and have to be expanded in a Laurent expansion around $\varepsilon = 0$, beginning at order $1/\varepsilon^3$, due to infrared divergences in the integrals. Fortunately, the IBP method also provides a way to determine the z-dependence of each coefficient in the Laurent expansion: Taking a derivative with respect to z produces an integral which can also be reduced to master integrals, thus generating a coupled set of differential equations [20] which are readily solved in terms of special functions. In this way the exact dependence of the NNLO partonic Higgs cross section on z was determined [18] (see also ref. [21]).

For the Drell-Yan or Higgs total cross section, the special functions that appear are polylogarithms of the form $\mathrm{Li}_n(z)$, defined by $\mathrm{Li}_1(z) = -\ln(1-z)$,

$$\mathrm{Li}_n(z) = \sum_{j=1}^{\infty} \frac{z^j}{j^n} = \int_0^z \frac{dt}{t} \mathrm{Li}_{n-1}(t)\,, \tag{2}$$

where $n \leq 3$, and the argument z may be replaced by a few other rational functions of

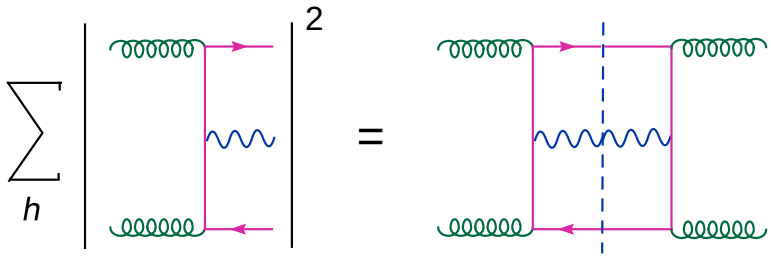

FIGURE 2. Unitarity relates the $gg \to V + X$ cross section to forward-scattering loop integrals.

z. The existence of the single scale z allows the analytical complexity, in terms of the number of different algebraic objects present, to grow significantly with respect to $R_{e^+e^-}$, but it is not yet out of hand.

In principle, no NNLO computation of a collider process is complete without an evolution of the parton distributions from low to high scales at the same NNLO accuracy. Last year saw the long-awaited completion of the NNLO corrections to the DGLAP evolution kernels for parton distribution functions [22], $P_{ij}(x)$. These were also computed by considering a forward scattering problem, with a virtual photon and a quark in the initial and final state. (For the gluon evolution kernel $P_{gg}(x)$, and also for $P_{qg}(x)$, a fictitious Higgs-like scalar ϕ, coupling to gluons via $\phi \mathrm{tr}(G_{\mu\nu}G^{\mu\nu})$, is used instead of a virtual photon.) After renormalization and subtraction of collinear divergences from lower loop orders, the NNLO evolution kernels are identified from the remaining $1/\varepsilon$ poles in the expression, which must be subtracted in the $\overline{\mathrm{MS}}$ scheme for defining parton distribution functions (or equivalently, leading twist operators). As a by-product of the computation, the finite, order ε^0 terms give the N^{3}LO contributions to the DIS structure function F_2 and the NNLO contribution to F_L [16].

For these results, somewhat more complicated special functions are required, such as $\mathrm{Li}_n(x)$ with $n = 4$ for $P_{ij}(x)$ and $n = 5$ for F_2 and F_L. However, the ordinary polylogarithms are not sufficient; a suitable generalization, harmonic polylogarithms [23], can be used instead. In fact, these computations were *not* performed in terms of the variable x, but rather the variable N appearing in the Mellin transform, $\tilde{f}(N) \equiv \int_0^1 dx\, x^{N-1}\, f(x)$. In N-space, the special functions that appear at NNLO are harmonic sums, such as the one-dimensional sum $S_k(N) = \sum_{i=1}^N i^{-k}$, and the multi-dimensional generalization of it,

$$S_{m,m_1,m_2,\ldots,m_k}(N) = \sum_{i=1}^{N} \frac{S_{m_1,m_2,\ldots,m_k}(i)}{i^m}\,. \tag{3}$$

Although it might appear that in Mellin-moment space a no-scale problem has been recovered, it is of course an infinite set of no-scale problems. Indeed, at fixed moment N, the program `MINCER` can be used to compute anomalous dimensions at NNLO for $N = 2,4,6,8,10$ [24] and even up to $N = 16$ [25]. However, for the case of arbitrary N, new integral reduction algorithms had to be developed [22].

Recently, the Mellin moments of the NNLO Drell-Yan and Higgs production cross sections were presented in terms of harmonic sums of the form (3) [26], putting the mathematical structure of the two types of NNLO one-scale problems discussed here on the same footing.

There have been important phenomenological applications of these one-scale results. Also taking into account the resummation of large threshold logarithms from multiple soft-gluon resummation, through next-to-next-to-leading logarithmic accuracy [27], the uncertainty on the total Higgs production cross section at the Tevatron and LHC has been considerably reduced, from perhaps 30–40% at NLO, to perhaps 10–20% at NNLO+NNLL. Some of the immediate phenomenological impact of the NNLO evolution kernels and coefficient functions on "DIS-driven" MRST parton fits [28] was discussed elsewhere at this meeting [3, 29].

Two or more scale problems

Although the total cross sections for inclusive Drell-Yan and Higgs production are now known relatively well theoretically, in practice such quantities are not measurable experimentally. Numerous experimental cuts must be imposed to extract a signal from the background, for example, cuts on the transverse momentum, rapidity, and isolation of leptons or photons visible in the final state. In an ideal world, a flexible hadron-level Monte Carlo program, accurate to NNLO, would allow the effects of such cuts to be assessed. However, even fixed-order computations of generic ("multi-scale") NNLO observables are not yet available.

A special case which can be handled in the style of the previous section is the distribution in rapidity Y_V of a Drell-Yan pair or a Higgs boson. The former process can be used to extract parton distribution information from fixed-target production, or monitor the "partonic luminosity" via W and Z production at the LHC [5], because at leading order it is proportional to $q(x_1)\bar{q}(x_2)$ with $x_{1,2} = (M_V/\sqrt{s})e^{\pm Y_V}$. Compared with the total cross section approach of ref. [18], a δ function needs to be inserted into the phase-space integration, of the form $\delta(Y - Y_V)$. The IBP method still works [30], reducing the phase-space integrals to a set of master integrals depending on z and $u = (x_1/x_2)e^{-2Y_V}$, which can again be determined by integrating differential equations. The NNLO results have much lengthier expressions than the one-scale answers. They involve polylogarithms with arguments which can be irrational functions of z and u, for example $\mathrm{Li}_2[(u-1-i\sqrt{(4u^2-z(1+u)^2)/z}/(2u)]$. The same stability of the perturbative series seen for the total W and Z production cross section at NNLO, holds also bin-by-bin in rapidity [30].

For problems with more than two scales, for example e^+e^- event shapes and generic hadron-collider processes, a flexible, fully numerical approach seems necessary. The major bottleneck at present comes in integrating contributions containing the emission of two extra partons, which have quite complicated singularities as momenta become soft and/or collinear. There has been important recent progress in this direction. For lack of space, and because these developments were described in another talk at this workshop, I refer the reader to that report [3].

TWISTOR SPINOFFS

There has been a great deal of recent interest in novel methods for evaluating QCD tree and loop amplitudes, stimulated by Witten's topological string in twistor space [4]. In general, it is possible to find compact representations for amplitudes for many external particles, and more efficient techniques for computing the amplitudes, by making full use of their analytic structure (which is sometimes hidden). Twistor space [31] is a kind of Fourier transform of the usual momentum-space representation of amplitudes. Very often, a Fourier transform can expose simplicity. Consider the time-dependence of the electric field $E(t)$ associated with light arriving from the Sun. It has a pretty random appearance. However, transforming to energy variables, $E(t) \to E(\omega) = \int dt e^{i\omega t} E(t)$, reveals spectral lines, from which the presence of helium in the Sun could be deduced.

The twistor transform is very well-suited for describing the scattering of massless particles. Traditional scattering variables are the four-momentum vectors k_i^μ — which are null vectors in the massless case, $k_i^2 = 0$ — and their Lorentz-invariant products, $s_{ij} = (k_i + k_j)^2 = 2k_i \cdot k_j$. We can trade the k_i^μ for spinor variables, the right- and left-handed, or $+$ and $-$ chirality, solutions to the Dirac equation, $u_\pm(k_i)$. A shorthand notation for the two-component (Weyl) versions of these spinors is,

$$(\lambda_i)_\alpha \equiv u_+(k_i), \qquad (\tilde{\lambda}_i)_{\dot{\alpha}} \equiv u_-(k_i). \tag{4}$$

The trade is possible thanks to the form of the positive-energy projector for massless spinors, $u(k)\bar{u}(k) = \not{k}$, or in two-component notation,

$$k_i^\mu (\sigma_\mu)_{\alpha\dot{\alpha}} = (\not{k}_i)_{\alpha\dot{\alpha}} = (\lambda_i)_\alpha (\tilde{\lambda}_i)_{\dot{\alpha}} \,. \tag{5}$$

Instead of Lorentz-invariant products, the natural variables for massless scattering are spinor inner-products [32], defined by

$$\langle j\, l\rangle = \varepsilon^{\alpha\beta} (\lambda_j)_\alpha (\lambda_l)_\beta = \bar{u}_-(k_j) u_+(k_l)\,, \qquad [j\, l] = \varepsilon^{\dot{\alpha}\dot{\beta}} (\tilde{\lambda}_j)_{\dot{\alpha}} (\tilde{\lambda}_l)_{\dot{\beta}} = \bar{u}_+(k_j) u_-(k_l)\,. \tag{6}$$

These products are the square roots of the Lorentz products, up to a phase ϕ,

$$\langle j\, l\rangle = \sqrt{s_{jl}}\, e^{i\phi_{jl}}\,, \qquad [j\, l] = \pm\sqrt{s_{jl}}\, e^{-i\phi_{jl}}\,. \tag{7}$$

The utility of these variables was recognized already in the 1980s. For example, the Parke-Taylor tree amplitudes [33, 34] are for the scattering of two negative-helicity gluons, labelled j and l, and $n-2$ positive-helicity gluons. They are termed "maximally helicity-violating" (MHV) amplitudes, because tree amplitudes with fewer (zero or one) negative-helicity gluons vanish. In terms of spinorial variables, they take a remarkably simple form for any n,

$$A_n^{\text{MHV}\,,jl} \equiv A_n^{\text{tree}}(1^+, 2^+, \ldots, j^-, \ldots, l^-, \ldots, n^+) = i \frac{\langle j\, l\rangle^4}{\langle 1\, 2\rangle \langle 2\, 3\rangle \cdots \langle n\, 1\rangle}\,, \tag{8}$$

depending only on the positive-helicity spinors λ_i, not the $\tilde{\lambda}_i$.

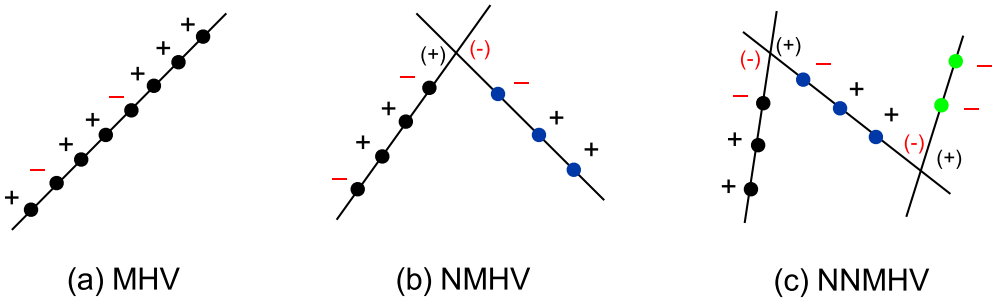

FIGURE 3. Tree amplitudes are supported on networks of intersecting lines in twistor space.

Twistor space and MHV rules

The twistor transform is a Fourier transform of the $\tilde{\lambda}_i$, leaving the λ_i alone. The four coordinates of twistor space, for each of the n particles, are $(\lambda_1, \lambda_2, \mu^{\dot{1}}, \mu^{\dot{2}})$, where $\mu^{\dot{\alpha}}$ is defined by

$$\tilde{\lambda}_{\dot{\alpha}} = i\frac{\partial}{\partial \mu^{\dot{\alpha}}}, \qquad \mu^{\dot{\alpha}} = i\frac{\partial}{\partial \tilde{\lambda}_{\dot{\alpha}}}. \tag{9}$$

In order to transform the MHV amplitudes (8), following ref. [4] we first must multiply them by the momentum-conserving δ-function, which can be written, using eq. (5) as,

$$\delta\Big(\sum_i k_i\Big) = \int d^4x \exp[ix^{\alpha\dot{\alpha}}(\lambda_i)_\alpha(\tilde{\lambda}_i)_{\dot{\alpha}}]. \tag{10}$$

Then the transformed amplitudes are

$$\tilde{A}_n^{\mathrm{MHV},jl}(\lambda_i,\mu_i) = \int \prod_i d\tilde{\lambda}_i \exp(i\mu_i\tilde{\lambda}_i) \int d^4x\, A(\lambda_i) \exp[ix\lambda_i\tilde{\lambda}_i] \propto \prod_i \delta(\mu_i + x\lambda_i). \tag{11}$$

The product of all the linear δ functions means that the amplitude is supported on a line in twistor space, as shown in fig. 3(a).

Investigation of amplitudes with three and four negative helicities (NMHV and NNMHV amplitudes) revealed the pattern of intersecting lines in fig. 3(b) and fig. 3(c). It also led to a set of "MHV rules" for QCD tree amplitudes, which are simpler than Feynman rules [35]. Each line in fig. 3 corresponds to an "MHV vertex", which is a clever off-shell continuation of the MHV amplitude (8), labelled with two negative helicities and the rest positive. Many Feynman vertices can be lumped effectively into a single MHV vertex. The MHV vertices are joined with scalar propagators, that is, factors of $1/p^2$, so that no messy contractions of Lorentz indices have to be performed. An example of an MHV-rules diagram, corresponding to the twistor-space structure in fig. 3(c), is given in fig. 4.

The efficiency of the MHV rules for gluonic amplitudes motivated their quick extension to amplitudes with massless external fermions [36], Higgs bosons coupling to gluons via $H\mathrm{tr}(G_{\mu\nu}G^{\mu\nu})$ in the large m_t limit [37], and vector bosons (γ^*, W, Z), including DIS multi-jet processes [38].

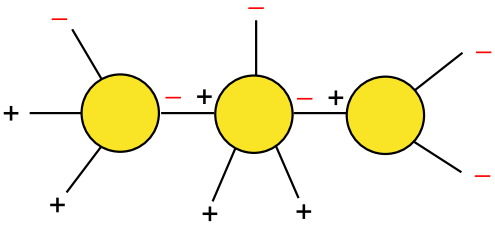

FIGURE 4. Example of an MHV-rules diagram, corresponding to fig. 3(c).

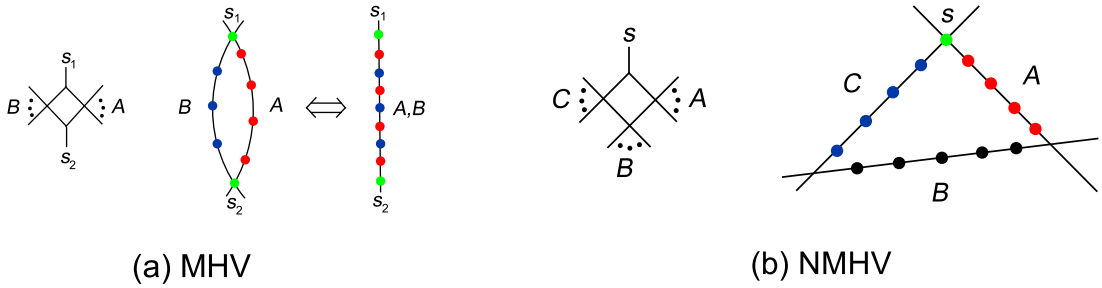

FIGURE 5. Twistor structure of box integral coefficients for one-loop amplitudes in $\mathcal{N}=4$ supersymmetric Yang-Mills theory.

In a parallel development, the twistor structure of loop amplitudes was explored and exploited [39]. The simplest structure to explain is for gluonic loop amplitudes in a computational "toy model" for QCD, maximally ($\mathcal{N}=4$) supersymmetric Yang-Mills theory. One-loop amplitudes in this theory can be written as a linear combination of scalar box integrals; no triangles or bubbles are required. The box integrals typically have many legs from the amplitude clustered into a single vertex of the box. In the MHV case, the coefficients of the boxes are either zero, or else equal to the MHV tree amplitudes $A_n^{\mathrm{MHV},jl}$ [40], in which case the vertices all lie on a single line in twistor space, as shown in fig. 5(a). However, this pattern turns out to be a degenerate case, which is resolved in the NMHV amplitudes. Here the simplest non-vanishing box coefficients are those with three clusters A,B,C and a single massless leg s. Their coefficients are supported on three lines intersecting in a ring, as shown in fig. 5(b) [41].

On-shell recursion relations

Quite recently, another approach to tree amplitudes has been developed, on-shell recursion relations [42, 43, 44]. These relations are somewhat more efficient and easier to generalize than the MHV rules [45], and they have very promising implications for loop amplitudes as well [46]. The derivation of the relations [44] is very general, relying just on Cauchy's theorem for functions of a single complex variable, and the factorization properties of amplitudes. The desired amplitude $A_n = A_n(0)$ can be embedded into a family of amplitudes $A_n(z)$, labelled by a complex parameter z characterizing a shift in the momentum flowing through the amplitude. For example, the momenta of the pair

of legs 1 and n can be shifted, while respecting overall momentum conservation and masslessness of the external legs, according to $k_1 \to \hat{k}_1(z)$, $k_n \to \hat{k}_n(z)$, where

$$\hat{k}_1(z) + \hat{k}_n(z) = k_1(z) + k_n(z), \qquad \hat{k}_1^2(z) = \hat{k}_n^2(z) = 0. \tag{12}$$

A momentum shift satisfying eq. (12) is best described using spinor variables, as

$$\lambda_1 \to \lambda_1 + z\lambda_n, \quad \tilde{\lambda}_1 \to \tilde{\lambda}_1; \qquad \lambda_n \to \lambda_n, \quad \tilde{\lambda}_n \to \tilde{\lambda}_n - z\tilde{\lambda}_1. \tag{13}$$

This is because a complex massless vector k^μ has $\det(\not{k}) = k^2 = 0$. So the singular 2×2 matrix $\not{k}$ can be factored into a pair of spinors, as $(\not{k})_{\alpha\dot{\alpha}} = \lambda_\alpha \tilde{\lambda}'_{\dot{\alpha}}$, as in eq. (5), where $\tilde{\lambda}'$ is no longer the conjugate spinor to λ.

As z varies over the complex plane, different intermediate states go on shell, generating poles in z. Let $K_{1,l} \equiv k_1 + k_2 + \cdots + k_l$. Then $\hat{K}_{1,l}^2(z) = (K_{1,l} + z\lambda_n\tilde{\lambda}_1)^2$ vanishes at

$$z = z_l = -K_{1,l}^2 / \langle n^- | \not{K}_{1,l} | 1^- \rangle \,. \tag{14}$$

So long as $A_n(z) \to 0$ as $z \to \infty$, the contour integral over a large circle C, $\frac{1}{2\pi i}\oint_C dz A_n(z)/z$ vanishes. The residue at $z = 0$, which is the desired amplitude $A_n(0)$, is the negative of the sum of the residues at $z = z_l$. Those residues are given by the factorization of the amplitude into two lower-point amplitudes, evaluated in shifted, on-shell kinematics. The resulting recursion relation [43] includes a sum over l, and over the possible intermedate helicities h,

$$A_n(1,2,\ldots,n) = \sum_{h=\pm}\sum_{l=2}^{n-2} A_{l+1}(\hat{1},2,\ldots,l,-\hat{K}_{1,l}^{-h}) \frac{i}{K_{1,l}^2} A_{n-l+1}(\hat{K}_{1,l}^{h}, l+1,\ldots,n-1,\hat{n}). \tag{15}$$

These relations lead quickly to very compact forms for tree amplitudes. For example, there are 220 Feynman diagrams for the six-gluon amplitude. Using color algebra and symmetries, the information in these diagrams is represented by the MHV amplitudes (8), plus two more helicity amplitudes, $A_6(1^+,2^+,3^+,4^-,5^-,6^-)$ and $A_6(1^+,2^+,3^-,4^+,5^-,6^-)$. Computing the first of them using the shift (13), yields the set of diagrams shown in fig. 6. Diagram (b) vanishes because $A_4(-,+,+,+) = 0$. Diagram (c) is related to diagram (a) by the symmetry $(1 \leftrightarrow 6, 2 \leftrightarrow 5, 3 \leftrightarrow 4)$ (plus spinor conjugation). Diagram (a) can be evaluated in a few steps, using the MHV amplitudes, to give a single-term expression. Adding diagram (c) gives,

$$\begin{aligned} -iA_6(1^+,2^+,3^+,4^-,5^-,6^-) \;&=\; \frac{\langle 6^-|(1+2)|3^-\rangle^3}{\langle 61\rangle\langle 12\rangle[34][45]s_{612}\langle 2^-|(6+1)|5^-\rangle} \\ &\quad + \frac{\langle 4^-|(5+6)|1^-\rangle^3}{\langle 23\rangle\langle 34\rangle[56][61]s_{561}\langle 2^-|(6+1)|5^-\rangle}\,. \end{aligned} \tag{16}$$

The combination $\langle 2^-|(6+1)|5^-\rangle = \langle 26\rangle[65] + \langle 21\rangle[15]$ in the denominator leads to an unphysical singularity in the first term of eq. (16) when $k_6 + k_1$ is a linear combination of k_2 and k_5, which is cancelled by the second term. On the other hand, all of the physical factorization behavior is made manifest, in contrast to Feynman-diagram

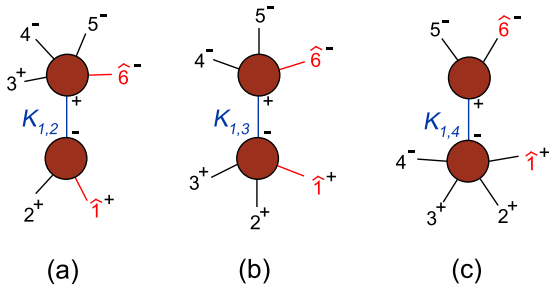

FIGURE 6. On-shell recursive diagrams for $A_6(1^+,2^+,3^+,4^-,5^-,6^-)$.

based representations [32]. The amplitude $A_6(1^+,2^+,3^-,4^+,5^-,6^-)$ has three independent recursive diagrams. Thus the six-gluon calculation is reduced from 220 Feynman diagrams to 4 much simpler ones.

The generality of this approach has led to its rapid application to different tree-level processes, with fermions and massive particles [45], and to one loop [46]. Essentially, amplitudes are being built up directly from their analytic properties. Considering that the heyday of *S*-matrix analyticity ended with the rise of a gauge theory for the strong interactions, QCD, these recent computational advances may herald the final revenge of the analytic *S*-matrix.

ACKNOWLEDGMENTS

I am grateful to the organizers of DIS 2005 for the invitation to present this talk, and for arranging such a stimulating meeting. I thank Zvi Bern, Vittorio Del Duca, Michael Klasen and David Kosower for helpful discussions. This work was supported by the US Department of Energy under contract DE–AC02–76SF00515.

REFERENCES

1. D. J. Gross and F. Wilczek, Phys. Rev. Lett. **30**, 1343 (1973); H. D. Politzer, Phys. Rev. Lett. **30**, 1346 (1973).
2. R. K. Ellis, H. Georgi, M. Machacek, H. D. Politzer and G. G. Ross, Nucl. Phys. B **152**, 285 (1979); A. H. Mueller, Phys. Rept. **73**, 237 (1981); J. C. Collins, D. E. Soper and G. Sterman, Nucl. Phys. B **261**, 104 (1985).
3. M. Klasen, these proceedings.
4. E. Witten, Commun. Math. Phys. **252**, 189 (2004) [hep-th/0312171].
5. M. Dittmar, F. Pauss and D. Zürcher, Phys. Rev. D **56**, 7284 (1997) [hep-ex/9705004].
6. S. G. Gorishnii, A. L. Kataev and S. A. Larin, Phys. Lett. B **259**, 144 (1991); L. R. Surguladze and M. A. Samuel, Phys. Rev. Lett. **66**, 560 (1991) [Erratum-ibid. **66**, 2416 (1991)].
7. S. A. Larin, F. V. Tkachov and J. A. M. Vermaseren, Phys. Rev. Lett. **66**, 862 (1991).
8. S. A. Larin and J. A. M. Vermaseren, Phys. Lett. B **259**, 345 (1991).
9. K. G. Chetyrkin and F. V. Tkachov, Nucl. Phys. B **192**, 159 (1981).
10. K. G. Chetyrkin and V. A. Smirnov, Phys. Lett. B **144**, 419 (1984).
11. S. G. Gorishnii, S. A. Larin, L. R. Surguladze and F. V. Tkachov, Comput. Phys. Commun. **55**, 381 (1989).
12. P. A. Baikov, K. G. Chetyrkin and J. H. Kuhn, Nucl. Phys. Proc. Suppl. **144**, 81 (2005).

13. S. Eidelman *et al.* [Particle Data Group], Phys. Lett. B **592**, 1 (2004).
14. R. Hamberg, W.L. van Neerven and T. Matsuura, Nucl. Phys. B **359**, 343 (1991) [Erratum-ibid. B **644**, 403 (2002)].
15. E.B. Zijlstra and W.L. van Neerven, Nucl. Phys. B **383**, 525 (1992).
16. J. A. M. Vermaseren, A. Vogt and S. Moch, hep-ph/0504242.
17. R. V. Harlander and W. B. Kilgore, Phys. Rev. Lett. **88**, 201801 (2002) [hep-ph/0201206].
18. C. Anastasiou and K. Melnikov, Nucl. Phys. B **646**, 220 (2002) [hep-ph/0207004].
19. S. Laporta, Int. J. Mod. Phys. A **15**, 5087 (2000) [hep-ph/0102033]; C. Anastasiou and A. Lazopoulos, JHEP **0407**, 046 (2004) [hep-ph/0404258].
20. T. Gehrmann and E. Remiddi, Nucl. Phys. B **580**, 485 (2000) [hep-ph/9912329].
21. V. Ravindran, J. Smith and W. L. van Neerven, Nucl. Phys. B **665**, 325 (2003) [hep-ph/0302135].
22. S. Moch, J. A. M. Vermaseren and A. Vogt, Nucl. Phys. B **688**, 101 (2004) [hep-ph/0403192]; Nucl. Phys. B **691**, 129 (2004) [hep-ph/0404111].
23. E. Remiddi and J. A. M. Vermaseren, Int. J. Mod. Phys. A **15**, 725 (2000) [hep-ph/9905237].
24. S. A. Larin, T. van Ritbergen and J. A. M. Vermaseren, Nucl. Phys. B **427**, 41 (1994); S. A. Larin, P. Nogueira, T. van Ritbergen and J. A. M. Vermaseren, Nucl. Phys. B **492**, 338 (1997) [hep-ph/9605317].
25. J. Blumlein and J. A. M. Vermaseren, Phys. Lett. B **606**, 130 (2005) [hep-ph/0411111].
26. J. Blumlein and V. Ravindran, Nucl. Phys. B **716**, 128 (2005) [hep-ph/0501178].
27. S. Catani, D. de Florian and M. Grazzini, JHEP **0105**, 025 (2001) [hep-ph/0102227]; S. Catani, D. de Florian, M. Grazzini and P. Nason, JHEP **0307**, 028 (2003) [hep-ph/0306211].
28. A. D. Martin, R. G. Roberts, W. J. Stirling and R. S. Thorne, Phys. Lett. B **604**, 61 (2004) [hep-ph/0410230].
29. R. S. Thorne, these proceedings.
30. C. Anastasiou, L. J. Dixon, K. Melnikov and F. Petriello, Phys. Rev. Lett. **91**, 182002 (2003) [hep-ph/0306192]; Phys. Rev. D **69**, 094008 (2004) [hep-ph/0312266].
31. R. Penrose, J. Math. Phys. 8:345 (1967).
32. M. L. Mangano and S. J. Parke, Phys. Rept. **200**, 301 (1991).
33. S. J. Parke and T. R. Taylor, Phys. Rev. Lett. 56:2459 (1986).
34. F. A. Berends and W. Giele, Nucl. Phys. B294:700 (1987); M. L. Mangano, S. J. Parke and Z. Xu, Nucl. Phys. B298:653 (1988).
35. F. Cachazo, P. Svrček and E. Witten, JHEP **0409**, 006 (2004) [hep-th/0403047].
36. G. Georgiou and V. V. Khoze, JHEP **0405**, 070 (2004) [hep-th/0404072]; J. B. Wu and C. J. Zhu, JHEP **0409**, 063 (2004) [hep-th/0406146]; G. Georgiou, E. W. N. Glover and V. V. Khoze, JHEP **0407**, 048 (2004) [hep-th/0407027].
37. L. J. Dixon, E. W. N. Glover and V. V. Khoze, JHEP **0412**, 015 (2004) [hep-th/0411092]; S. D. Badger, E. W. N. Glover and V. V. Khoze, JHEP **0503**, 023 (2005) [hep-th/0412275].
38. Z. Bern, D. Forde, D. A. Kosower and P. Mastrolia, hep-ph/0412167.
39. A. Brandhuber, B. Spence and G. Travaglini, Nucl. Phys. B **706**, 150 (2005) [hep-th/0407214]; F. Cachazo, P. Svrček and E. Witten, JHEP **0410**, 077 (2004) [hep-th/0409245]; R. Britto, F. Cachazo and B. Feng, Phys. Rev. D **71**, 025012 (2005) [hep-th/0410179]; S. J. Bidder, N. E. J. Bjerrum-Bohr, L. J. Dixon and D. C. Dunbar, Phys. Lett. B **606**, 189 (2005) [hep-th/0410296]; S. J. Bidder, N. E. J. Bjerrum-Bohr, D. C. Dunbar and W. B. Perkins, Phys. Lett. B **608**, 151 (2005) [hep-th/0412023].
40. Z. Bern, L. J. Dixon, D. C. Dunbar and D. A. Kosower, Nucl. Phys. B **425**, 217 (1994) [hep-ph/9403226].
41. Z. Bern, L. J. Dixon and D. A. Kosower, hep-th/0412210.
42. R. Roiban, M. Spradlin and A. Volovich, Phys. Rev. Lett. **94**, 102002 (2005) [hep-th/0412265].
43. R. Britto, F. Cachazo and B. Feng, Nucl. Phys. B **715**, 499 (2005) [hep-th/0412308].
44. R. Britto, F. Cachazo, B. Feng and E. Witten, Phys. Rev. Lett. **94**, 181602 (2005) [hep-th/0501052].
45. M. Luo and C. k. Wen, JHEP **0503**, 004 (2005) [hep-th/0501121]; Phys. Rev. D **71**, 091501 (2005) [hep-th/0502009]; R. Britto, B. Feng, R. Roiban, M. Spradlin and A. Volovich, Phys. Rev. D **71**, 105017 (2005) [hep-th/0503198]; S. D. Badger, E. W. N. Glover, V. V. Khoze and P. Svrcek, hep-th/0504159.
46. Z. Bern, L. J. Dixon and D. A. Kosower, Phys. Rev. D **71**, 105013 (2005) [hep-th/0501240]; hep-ph/0505055.